

Skewness, kurtosis, 5th and 6th order cumulants of conserved charge fluctuations and the comparison to STAR data



Christian Schmidt
HotQCD Collaboration



HotQCD Collaboration

A. Bazavov, D. Bollweg, H.-T. Ding, P. Enns, J. Goswami, P. Hegde, O. Kaczmarek, F. Karsch, A. Lahiri, S.-T. Li, Swagato Mukherjee, H. Ohno, P. Petreczky, C. Schmidt, S. Sharma, P. Steinbrecher,

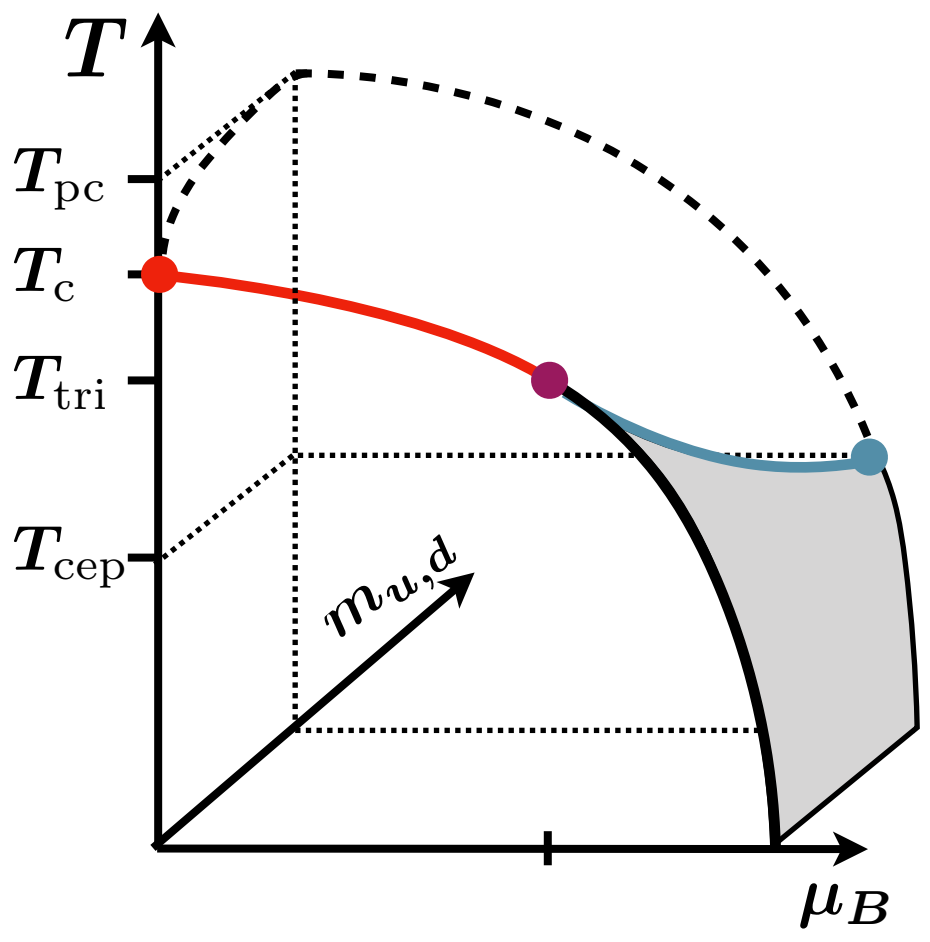
→ See also QM'19 talk by D. Bollweg

Workshop on QCD in the Nonperturbative Regime,
18-20 Nov 2019, TIFR, Mumbai, India

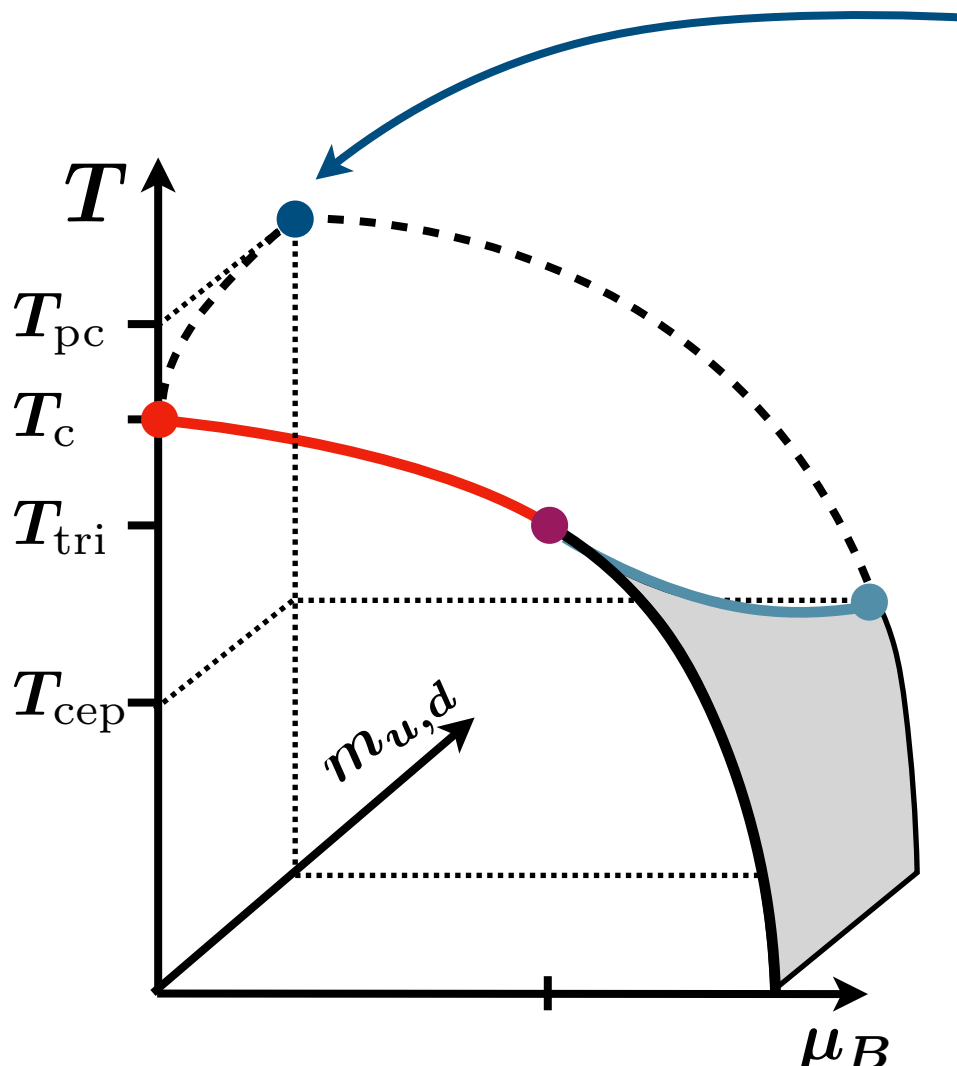


Tata Institute of Fundamental Research
टाटा मूलभूत अनुसंधान संस्थान

Motivation: The QCD Phase diagram



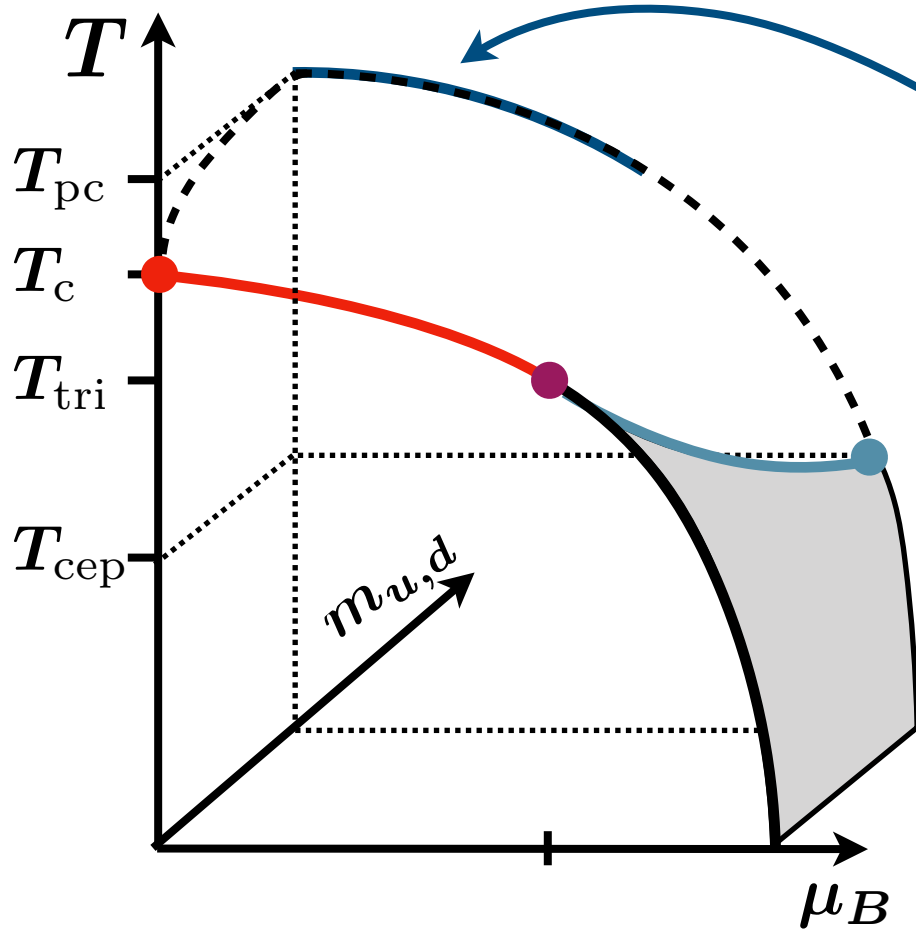
Motivation: The QCD Phase diagram



- New precise determination of the QCD transition temperature $T_{pc} = 156.5 \pm 1.5$ MeV

HotQCD: PLB 795 (2019) 15

Motivation: The QCD Phase diagram



- New precise determination of the QCD transition temperature $T_{pc} = 156.5 \pm 1.5$ MeV

HotQCD: PLB 795 (2019) 15

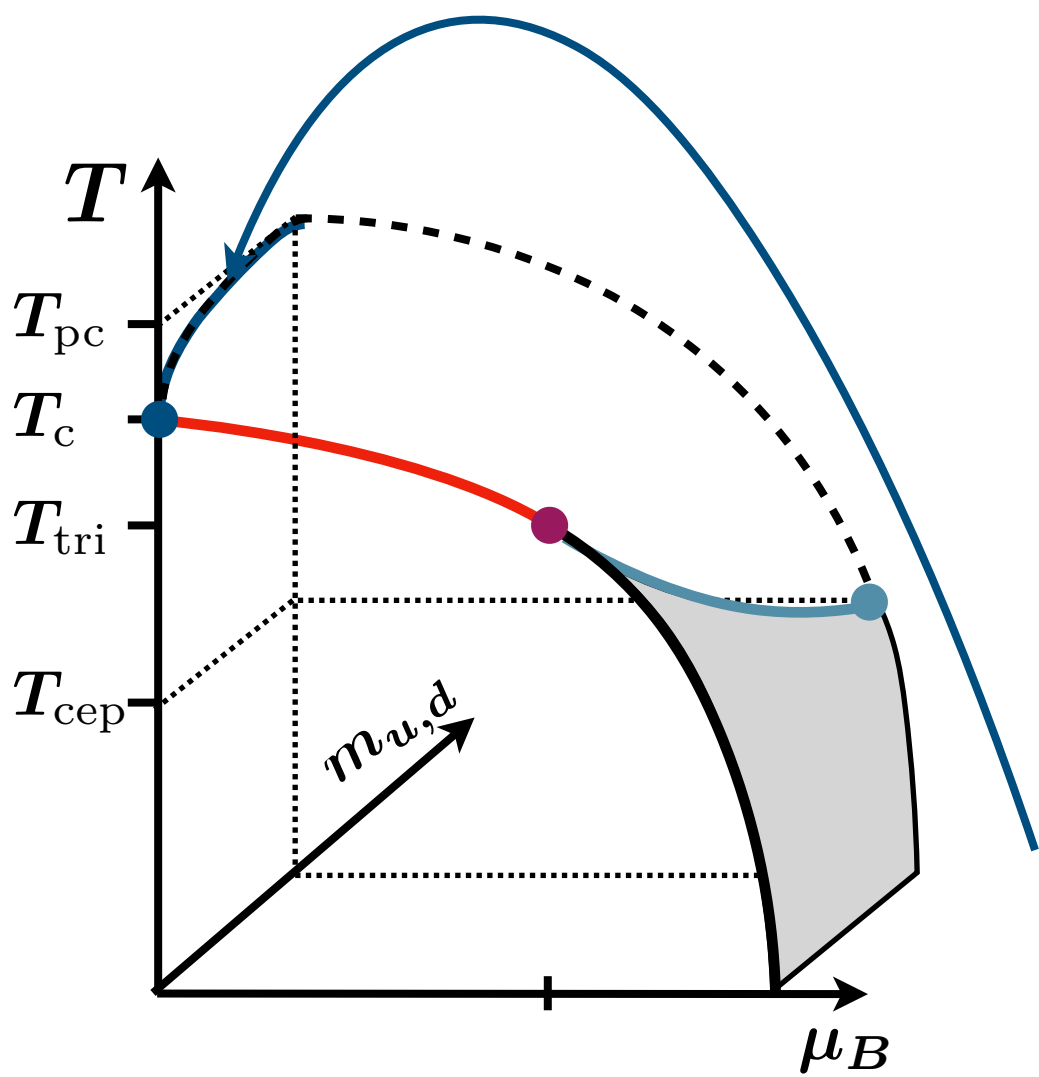
- The chiral crossover line with respect to μ_B

$$T_{pc}(\mu_B) = T_{pc}^0 \left(1 - \kappa_2^{B,f} \left(\frac{\mu_B}{T_{pc}^0} \right)^2 - \kappa_4^{B,f} \left(\frac{\mu_B}{T_{pc}^0} \right)^4 \right)$$

$$\kappa_2^{B,f} = 0.012(4), \quad \kappa_4^{B,f} = 0.00(4)$$

HotQCD: PLB 795 (2019) 15

Motivation: The QCD Phase diagram



- New precise determination of the QCD transition temperature $T_{pc} = 156.5 \pm 1.5$ MeV

HotQCD: PLB 795 (2019) 15

- The chiral crossover line with respect to μ_B

$$T_{pc}(\mu_B) = T_{pc}^0 \left(1 - \kappa_2^{B,f} \left(\frac{\mu_B}{T_{pc}^0} \right)^2 - \kappa_4^{B,f} \left(\frac{\mu_B}{T_{pc}^0} \right)^4 \right)$$

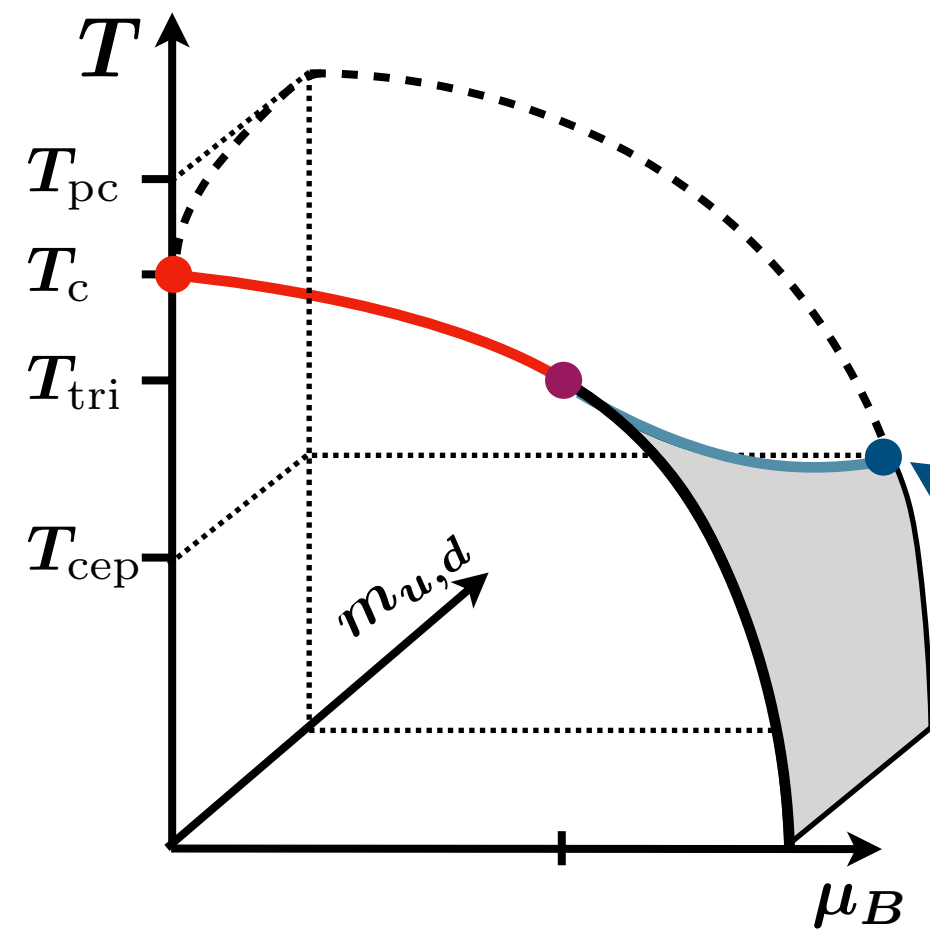
$$\kappa_2^{B,f} = 0.012(4), \quad \kappa_4^{B,f} = 0.00(4)$$

HotQCD: PLB 795 (2019) 15

- The chiral phase transition temperature and pseudo-critical line $T_c = 132_{-6}^{+3}$ MeV

HotQCD: PRL 123 (2019) 062002

Motivation: The QCD Phase diagram



- New precise determination of the QCD transition temperature $T_{pc} = 156.5 \pm 1.5$ MeV

HotQCD: PLB 795 (2019) 15

- The chiral crossover line with respect to μ_B

$$T_{pc}(\mu_B) = T_{pc}^0 \left(1 - \kappa_2^{B,f} \left(\frac{\mu_B}{T_{pc}^0} \right)^2 - \kappa_4^{B,f} \left(\frac{\mu_B}{T_{pc}^0} \right)^4 \right)$$

$$\kappa_2^{B,f} = 0.012(4), \quad \kappa_4^{B,f} = 0.00(4)$$

HotQCD: PLB 795 (2019) 15

- The chiral phase transition temperature and pseudo-critical line $T_c = 132_{-6}^{+3}$ MeV

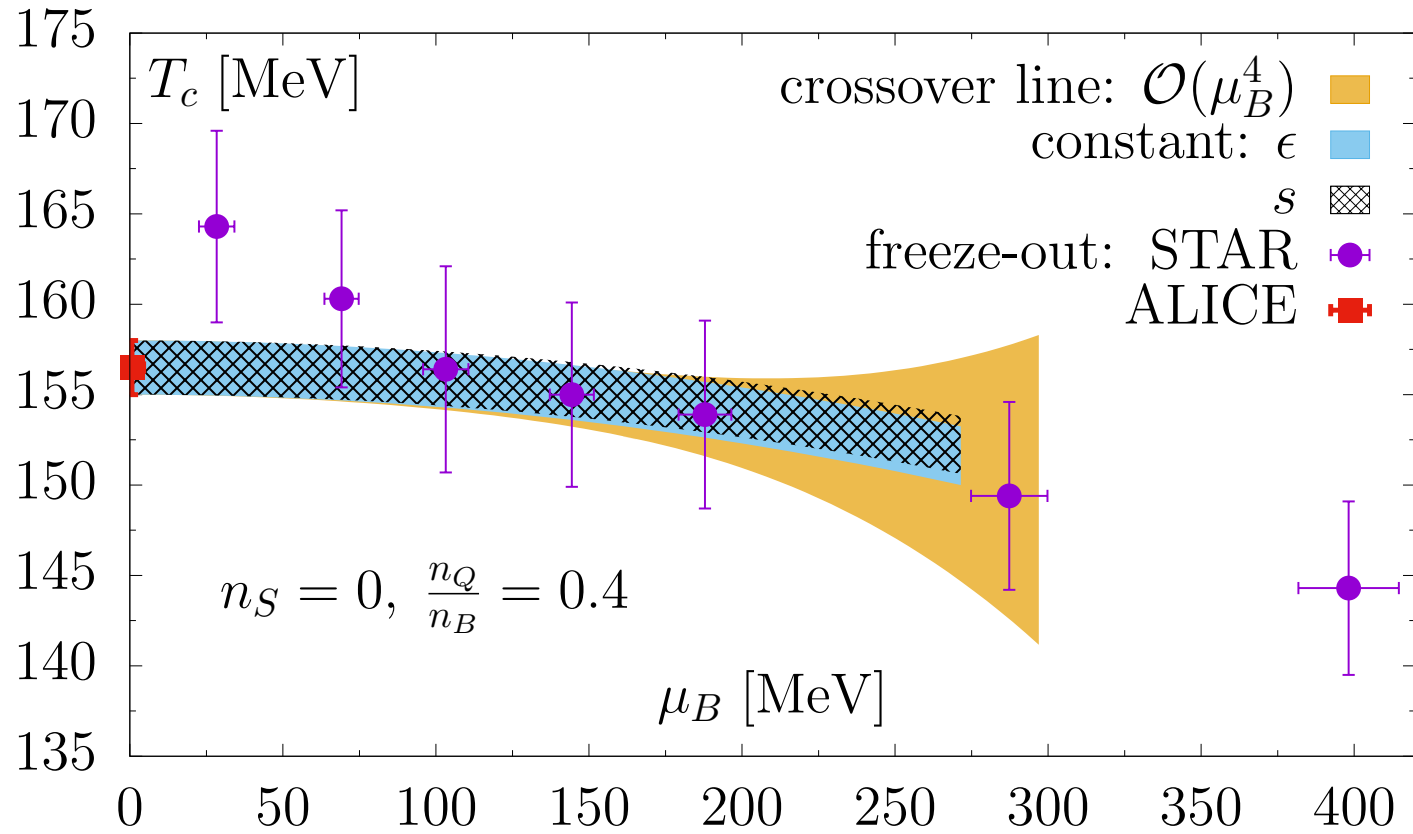
HotQCD: PRL 123 (2019) 062002

- Expected bounds on the QCD critical end-point

$$T_{cep} < T_c = 132_{-6}^{+3} \text{ MeV}$$

$$\mu_B^{cep} > (300 - 400) \text{ MeV}$$

Motivation: Freeze-out data vs. lattice QCD



- Established Method to extract freeze-out parameter from HIC experiments uses hadronic yields and fits to a statistical (HRG) model.

- ➔ Find good agreement with the chiral crossover line from QCD
- ➔ Model dependent analysis
- ➔ No phase transition in the HRG

- Higher order cumulants of conserved charge fluctuations are the ideal probes to study the freeze-out and chiral crossover line.
 - ➔ Can be calculated in (lattice) QCD
 - ➔ Show well defined divergencies close to the critical end-point and extrema at the chiral crossover

Goal: Provide QCD predictions for cumulant ratios (M/σ^2 , $S\sigma$, $\kappa\sigma^2$, ...) of conserved charge fluctuations as net baryon-number (B), net electric charge (Q), net strangeness (S).

- **Methodology**
 - ▶ Definition of cumulant ratios
 - ▶ Formulation of observables on the lattice
 - ▶ Recent improvements
- **Results: A comparison to HRG**
 - ▶ Using HRG to estimate difference of net-baryon and net-proton number fluctuations (only M/σ^2)
- **Results: A comparison to STAR**
 - ▶ Thermodynamic consistency of the new $\sqrt{s_{NN}} = 54.4$ GeV proton-number fluctuations
- **Summary and Outlook**

Methodology: The Taylor expansion method

- Compute expansion coefficients of the pressure

$$\frac{p}{T^4} = \frac{\ln Z}{T^3 V} = \sum_{i,j,k=0}^{\infty} \frac{1}{i!j!k!} \chi_{ijk,0}^{BQS} \left(\frac{\mu_B}{T}\right)^i \left(\frac{\mu_Q}{T}\right)^j \left(\frac{\mu_S}{T}\right)^k$$

Gavai, Gupta (2001)
Bielefeld-Swansea (2002)

Cumulants of conserved charge fluctuations, can also be measured as event-by-event fluctuations in heavy ion collisions

$$\chi_{ijk,0}^{BQS} = \frac{\partial^i}{\partial(\mu_B/T)} \frac{\partial^j}{\partial(\mu_Q/T)} \frac{\partial^k}{\partial(\mu_S/T)} \frac{\ln Z}{T^3 V}$$

Methodology: The Taylor expansion method

- Compute expansion coefficients of the pressure

$$\frac{p}{T^4} = \frac{\ln Z}{T^3 V} = \sum_{i,j,k=0}^{\infty} \frac{1}{i!j!k!} \chi_{ijk,0}^{BQS} \left(\frac{\mu_B}{T}\right)^i \left(\frac{\mu_Q}{T}\right)^j \left(\frac{\mu_S}{T}\right)^k$$

Gavai, Gupta (2001)
Bielefeld-Swansea (2002)

- **Notation:** relevant operators are derivatives of the determinant

$$D_i^f = \frac{\partial^i}{\partial \mu_f^i} \det [M_f(\mu_f)]^{1/4} = \frac{\partial^i}{\partial \mu_f^i} e^{\frac{1}{4} \text{Tr} \ln M_f(\mu_f)}, \quad f \in \{u, d, s\}$$

up to 4th-order in μ :

exponential dependence:

$$\begin{aligned} D_1^f &= \text{Tr} \left[M_f^{-1} M_f^{(1)} \right] \\ D_2^f &= -\text{Tr} \left[M_f^{-1} M_f^{(1)} M_f^{-1} M_f^{(1)} \right] \\ &\quad + \text{Tr} \left[M_f^{-1} M_f^{(2)} \right] \\ &\quad \vdots \end{aligned}$$

from 6th-order in μ onwards:

linear dependence:

$$\begin{aligned} D_1^f &= \text{Tr} \left[M_f^{-1} M_f^{(1)} \right] \\ D_2^f &= -\text{Tr} \left[M_f^{-1} M_f^{(1)} M_f^{-1} M_f^{(1)} \right] \end{aligned}$$

all $M_f^{(k)} = 0$, for $k > 1$

⇒ much less operators to measure!

Gavai, Sharma 2015

Methodology: The Taylor expansion method

- Compute expansion coefficients of the pressure

$$\frac{p}{T^4} = \frac{\ln Z}{T^3 V} = \sum_{i,j,k=0}^{\infty} \frac{1}{i!j!k!} \chi_{ijk,0}^{BQS} \left(\frac{\mu_B}{T}\right)^i \left(\frac{\mu_Q}{T}\right)^j \left(\frac{\mu_S}{T}\right)^k$$

Gavai, Gupta (2001)
Bielefeld-Swansea (2002)

- Interpretation:

$$\begin{aligned} \chi_{200}^{uds} &= \frac{\partial^2}{\partial(\mu_u/T)^2} \left(\frac{\ln Z}{T^3 V}\right) = \langle D_2^u \rangle + \langle (D_1^u)^2 \rangle \\ &= \langle \text{Tr} [M_u^{-1} M_u^{(2)}] \rangle - \langle \text{Tr} [M_u^{-1} M_u^{(1)} M_u^{-1} M_u^{(1)}] \rangle \\ &\quad + \langle \text{Tr} [M_u^{-1} M_u^{(1)}] \text{Tr} [M_u^{-1} M_u^{(1)}] \rangle \\ &= \langle \text{Diagram 1} \rangle - \langle \text{Diagram 2} \rangle + \langle \text{Diagram 3} \rangle \end{aligned}$$

$$\text{Diagram 1} = [M_f^{-1} M_f^{(1)}]_{xx}$$

$f \triangleq$ local f-quark density

$$\text{Diagram 2} = [M_f^{-1} M_f^{(2)}]_{xx}$$

$f \triangleq$ un-physical contact term

Methodology: The Taylor expansion method

- **Random noise method:**

- Choose a number of random vectors $\eta^{(k)}$ with
- The trace of a matrix A is approximated as

$$\lim_{N \rightarrow \infty} \frac{1}{N} \sum_k \eta_i^{(k)} \cdot \eta_j^{(k)} = \delta_{ij}$$

$$\text{Tr} A \approx \frac{1}{N} \sum_k \eta^{(k)\dagger} A \eta^{(k)}$$

$$\text{std} [\text{Tr} A] \sim \frac{1}{\sqrt{N}}$$

$\Rightarrow A := M^{-1}$: matrix inversion can be reduced to a linear problem $Mx = \eta$.

- **Unbiased estimators:**

- Need unbiased estimators for powers of traces: $(\text{Tr} A)^m$

$$(\text{Tr} A)^m \approx \frac{1}{\mathcal{N}} \sum_{k_1 \neq k_2, \dots \neq k_m} \left(\eta^{(k_1)\dagger} A \eta^{(k_1)} \right) \cdot \left(\eta^{(k_2)\dagger} A \eta^{(k_2)} \right) \dots \left(\eta^{(k_m)\dagger} A \eta^{(k_m)} \right)$$

\Rightarrow need at least m random vectors, more might be necessary to improve precision
(signal to noise ratio can be large)

\Rightarrow have developed efficient recursive method to calculate unbiased estimators

Methodology: Cumulant ratios of conserved charge fluctuations

- Combine quark number fluctuations (χ_{ijk}^{uds}) to obtain hadronic fluctuations (χ_{ijk}^{BQS}).
- Determine strangeness (μ_S/T) and electric charge chemical (μ_Q/T) potentials by imposing strangeness neutrality $n_S = 0$ and $n_Q/n_B = 0.4$ (order by order in the expansion).

- From the pressure expansion we readily obtain the expansions for the n^{th} -order cumulants:

$$\chi_n^B(T, \mu_B) = \sum_{k=0}^{k_{\max}} \tilde{\chi}_n^{B,k}(T) \hat{\mu}_B^k, \quad \text{with} \quad \hat{\mu}_B = \mu_B/T$$

- Define ratios to eliminate the leading order volume dependence

$$R_{nm}^B = \frac{\chi_n^B(T, \mu_B)}{\chi_m^B(T, \mu_B)} = \frac{\sum_{k=0}^{k_{\max}} \tilde{\chi}_n^{B,k}(T) \hat{\mu}_B^k}{\sum_{l=0}^{l_{\max}} \tilde{\chi}_m^{B,l}(T) \hat{\mu}_B^l}$$

- In terms of the shape parameters of the distribution we find

$$R_{12} = M/\sigma^2, \quad R_{31} = S\sigma^3/M, \quad R_{32} = S\sigma, \quad R_{42} = \kappa\sigma^2, \quad \dots$$

- Eventually we want calculate observables along the crossover (and freeze-out) line, we thus need spline interpolations of our data at discrete temperature values.

Methodology: Lattice setup and statistics

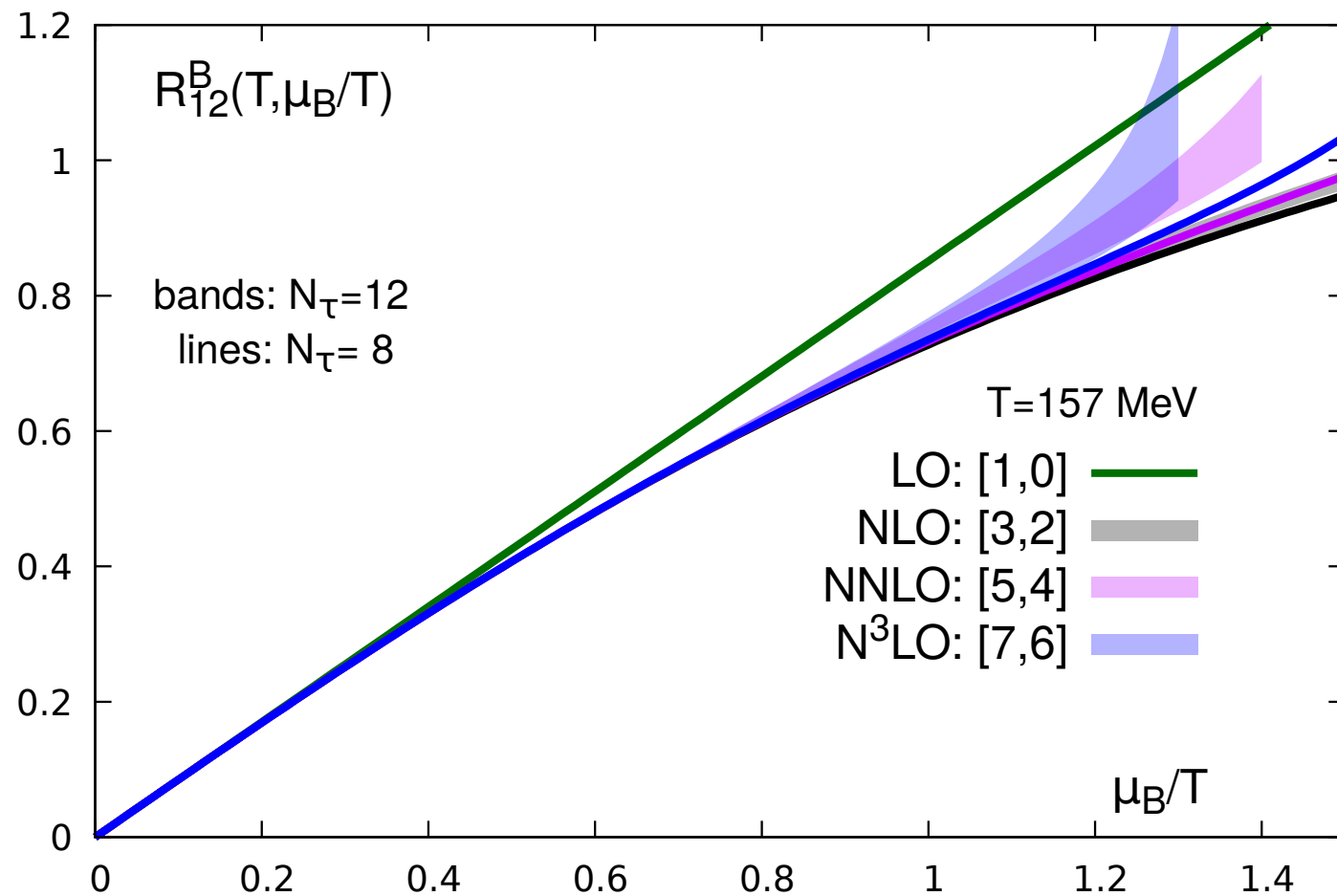
- Use (2+1)-flavor of HISQ-fermions, with physical strange and light quark masses.
- **Lattices sizes** are $32^3 \times 8$, $48^3 \times 12$, $64^3 \times 16$, at 9 different temperature values.
- **Statistics:** Compared to our previous analysis of skewness and kurtosis [[HotQCD, PRD 96 \(2017\) 074510](#)] we increased the statistics on ($N_\tau = 8$)-lattices by a factor 3-4 and on ($N_\tau = 12$)-lattices by a factor 6-8. I.e. we have now

N_τ	8	12	16
#conf.	$1.2 \cdot 10^6$	$(2 - 3) \cdot 10^5$	10^4

- **Order of the expansion:** We can now go to N³LO, compared to NLO in our previous study. I.e., we include 8-th order expansion coefficients of the pressure.
- This years calculations were performed on Summit, using Nvidia's V100 GPU's.

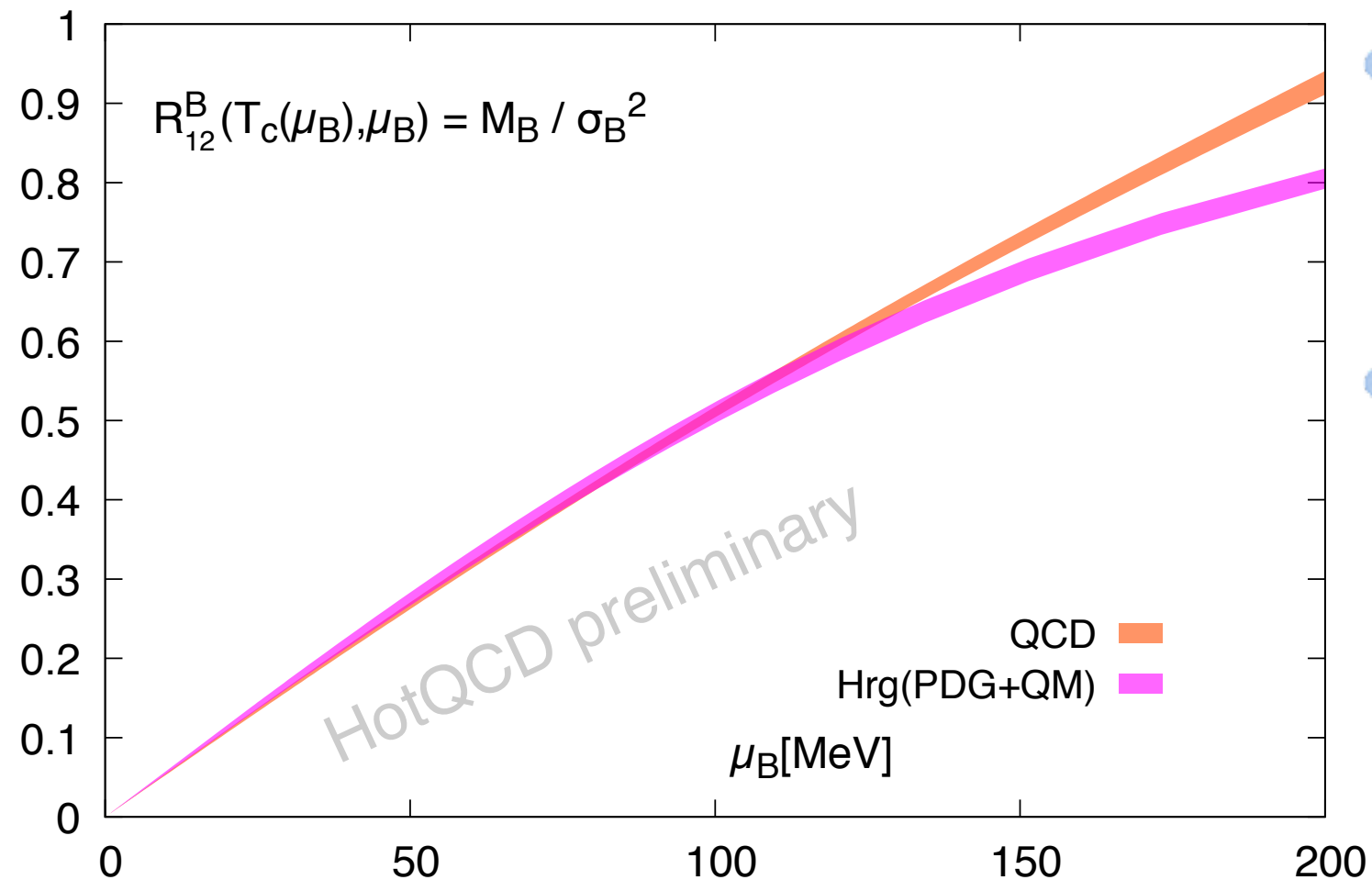


Results: The net baryon-number density R_{12}^B



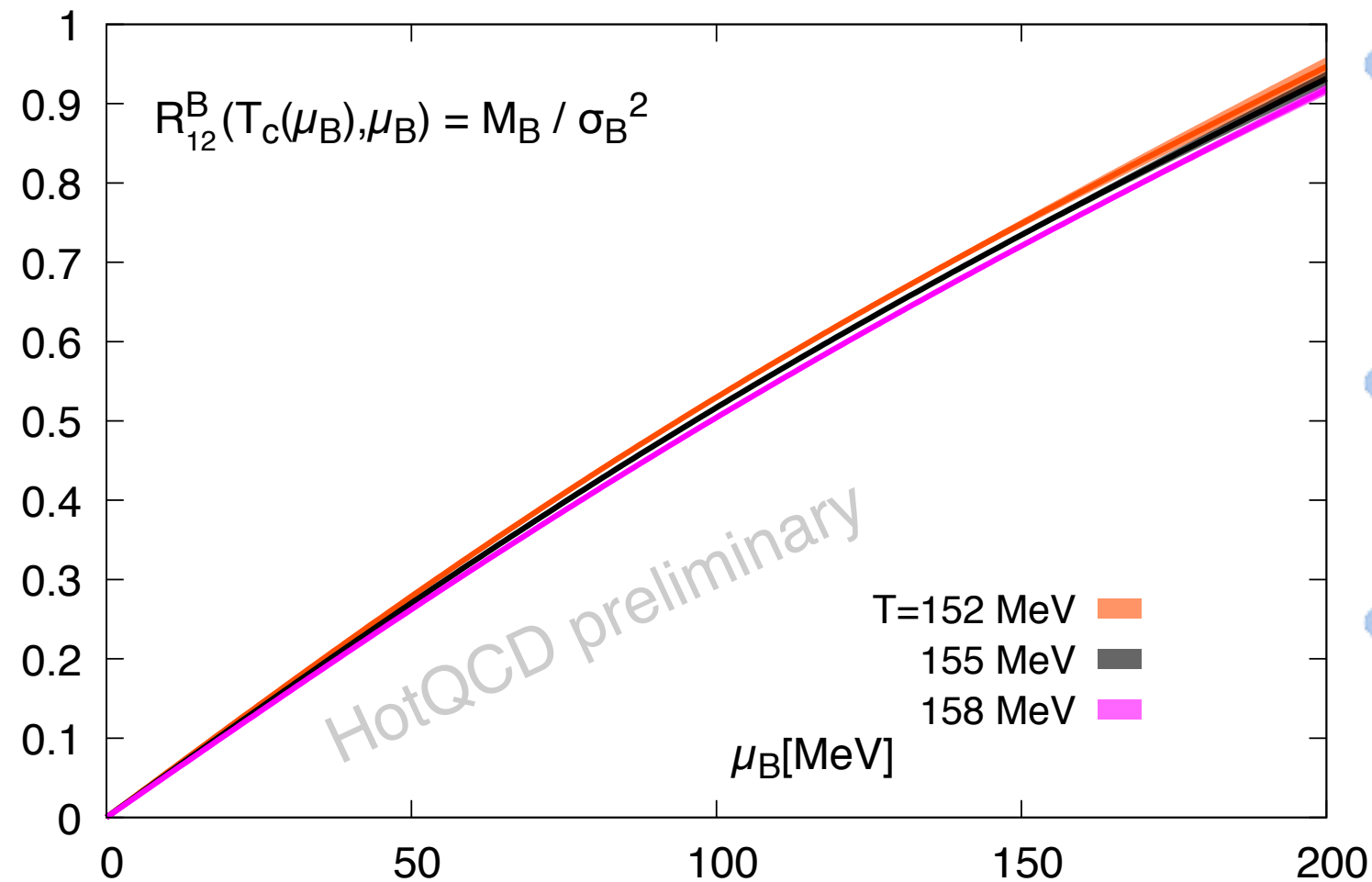
- Cut-off effects are negligible for $\mu_B/T \leq 1$ and of the same order as the statistical error at $N_\tau = 12$ for $\mu_B/T \leq 1.2$.

Results: The net baryon-number density R_{12}^B



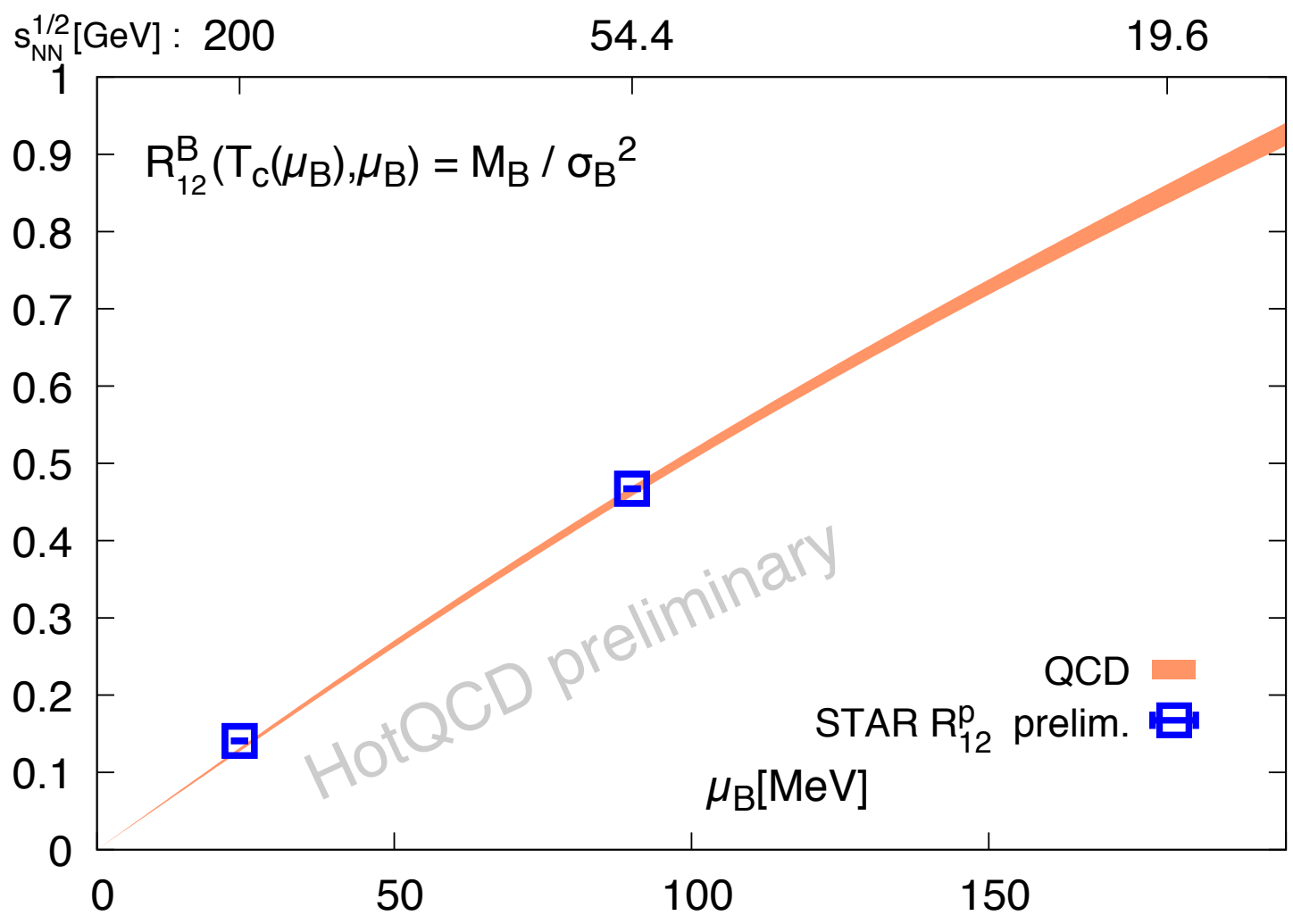
- Cut-off effects are negligible for $\mu_B/T \leq 1$ and of the same order as the statistical error at $N_\tau = 12$ for $\mu_B/T \leq 1.2$.
- Continuum extrapolation along the freeze-out line: good agreement with HRG (PDG+QM) up to $\mu_B \leq 120$ MeV

Results: The net baryon-number density R_{12}^B



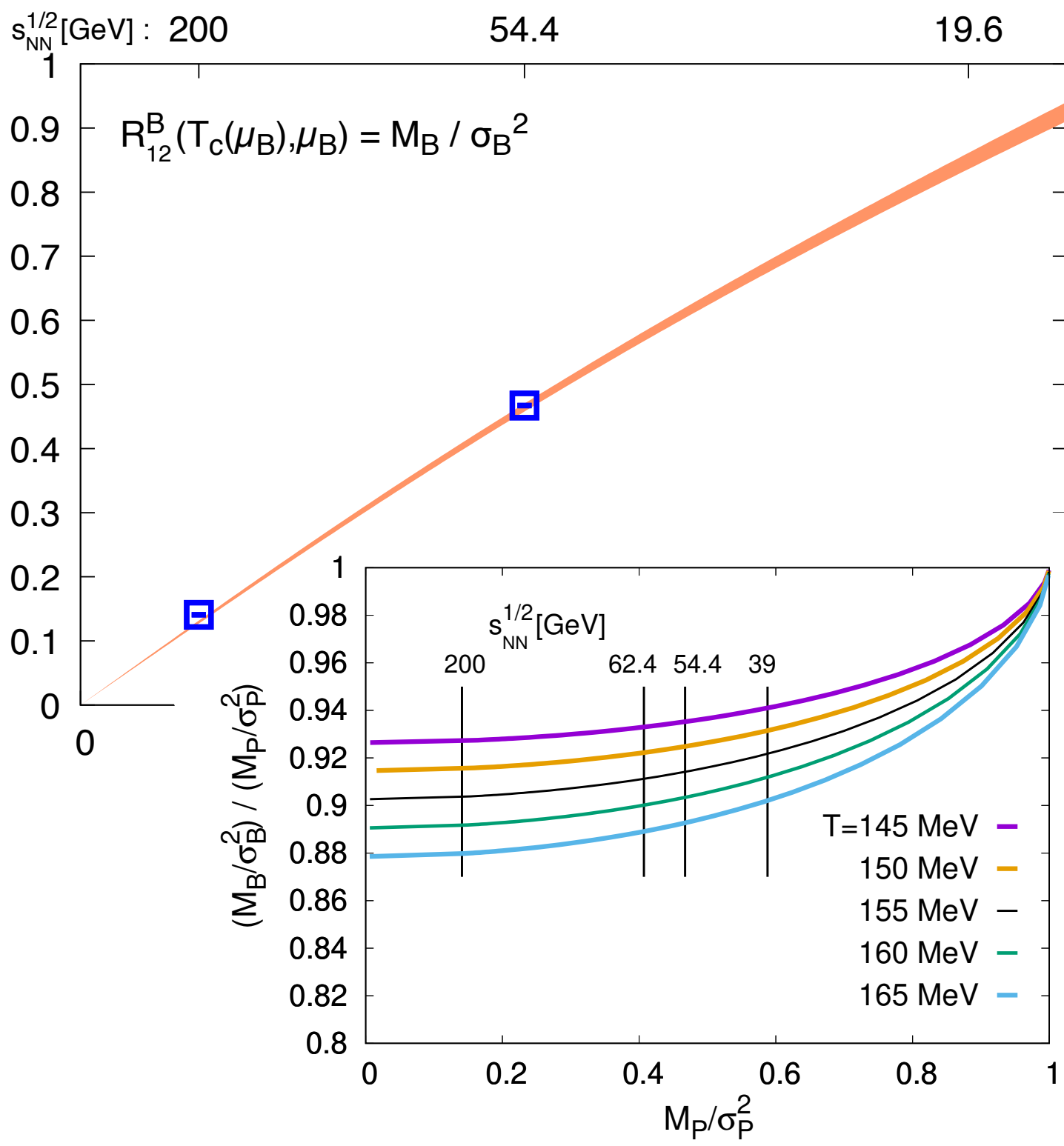
- Cut-off effects are negligible for $\mu_B/T \leq 1$ and of the same order as the statistical error at $N_\tau = 12$ for $\mu_B/T \leq 1.2$.
- Continuum extrapolation along the freeze-out line: good agreement with HRG (PDG+QM) up to $\mu_B \leq 120$ MeV
- Temperature dependence is very mild. The curvature of the freeze-out line varies the temperature by less than 3 MeV.

Results: The net baryon-number density R_{12}^B



- Cut-off effects are negligible for $\mu_B/T \leq 1$ and of the same order as the statistical error at $N_\tau = 12$ for $\mu_B/T \leq 1.2$.
- Continuum extrapolation along the freeze-out line: good agreement with HRG (PDG+QM) up to $\mu_B \leq 120$ MeV
- Temperature dependence is very mild. The curvature of the freeze-out line varies the temperature by less than 3 MeV.
- R_{12}^B may be used to eliminate μ_B in studies of higher order cumulants

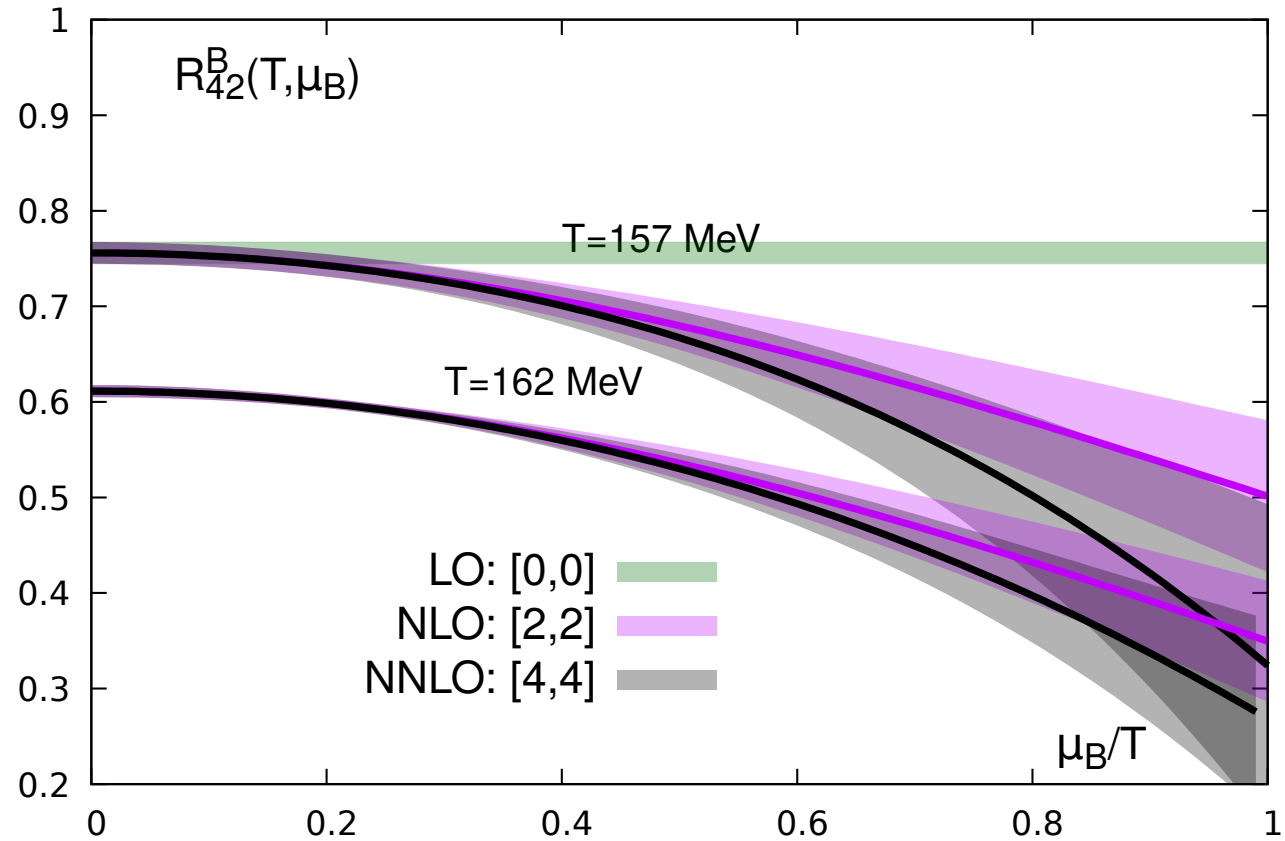
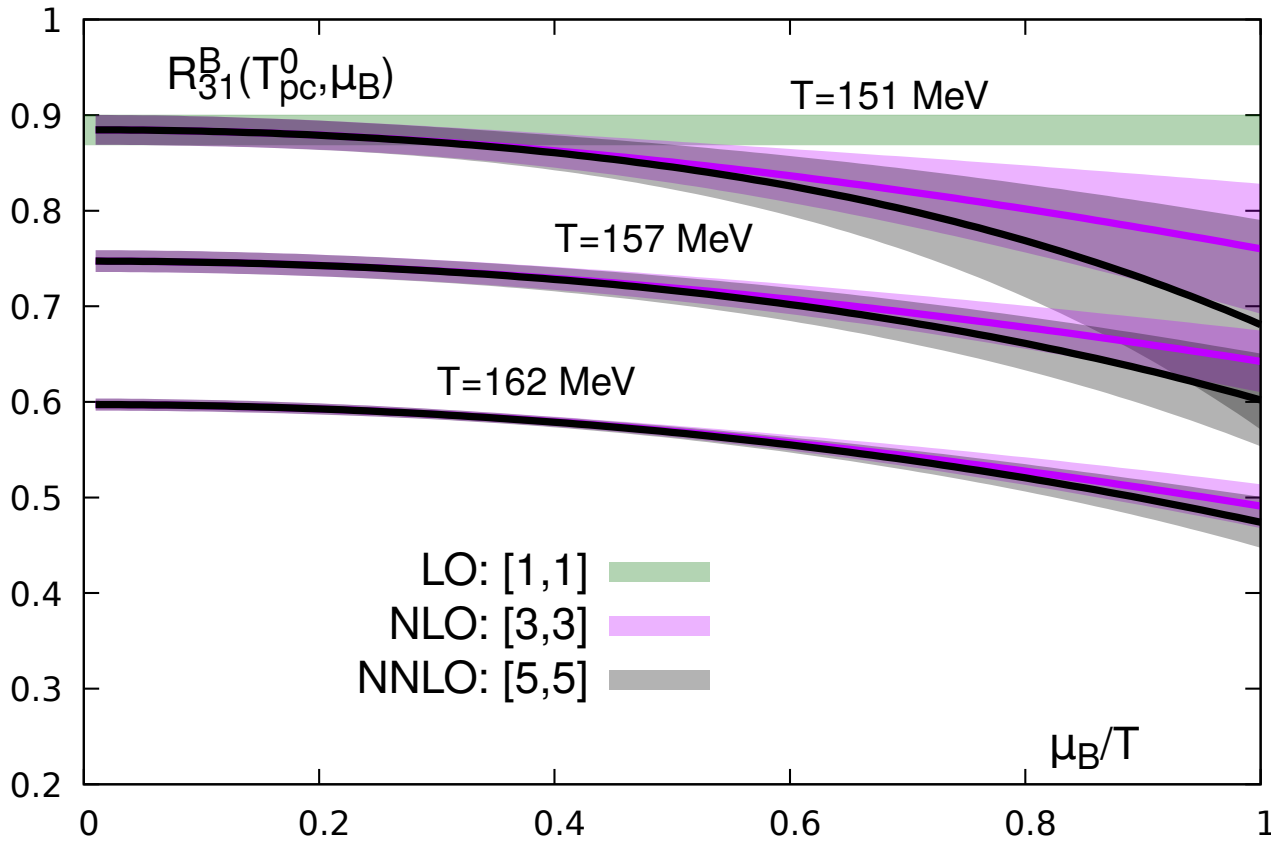
Results: The net baryon-number density R_{12}^B



- Cut-off effects are negligible for $\mu_B / T \leq 1$ and of the same order as the statistical error at $N_\tau = 12$ for $\mu_B / T \leq 1.2$.
- Continuum extrapolation along the freeze-out line: good agreement with HRG (PDG+QM) up to $\mu_B \leq 120$ MeV
- Temperature dependence is very mild. The curvature of the freeze-out line varies the temperature by less than 3 MeV.
- R_{12}^B may be used to eliminate μ_B in studies of higher order cumulants
- The difference of R_{12}^B and R_{12}^P is less than 10% in the HRG, one may or may not account for this difference in the determination of μ_B .

Results: Skewness and kurtosis

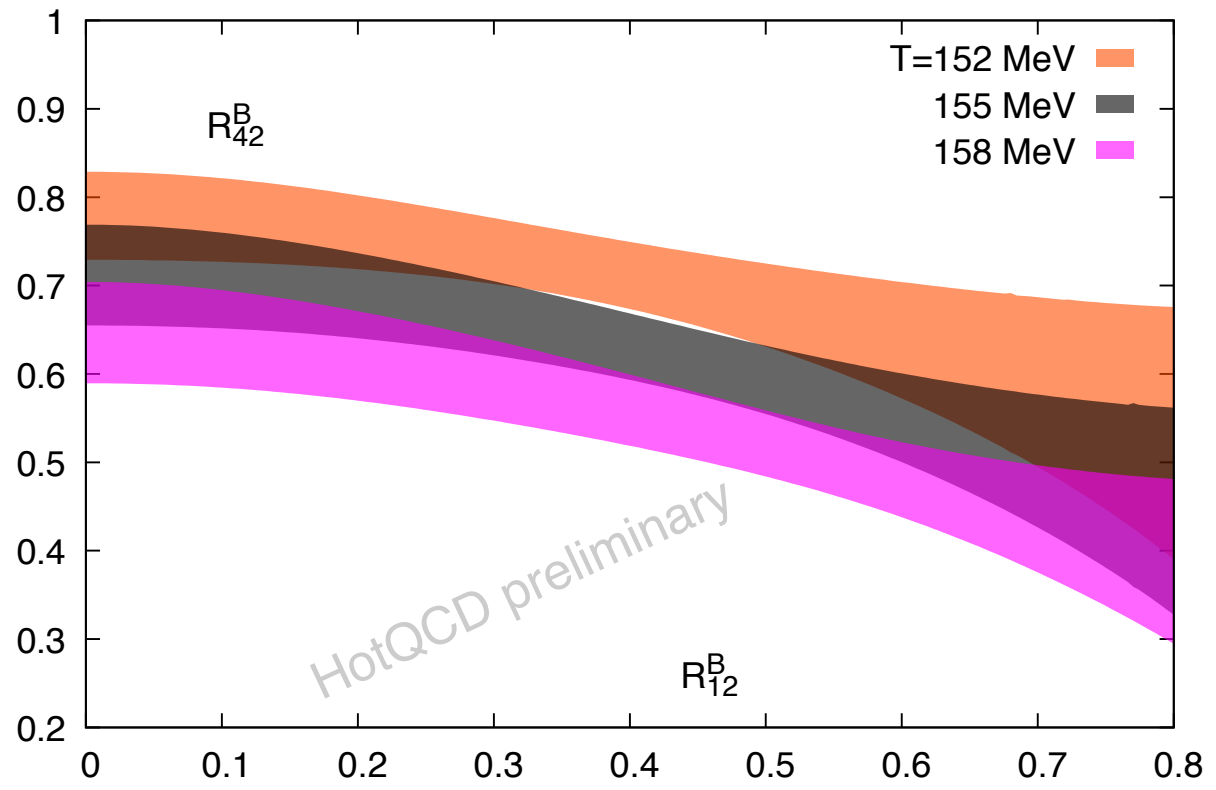
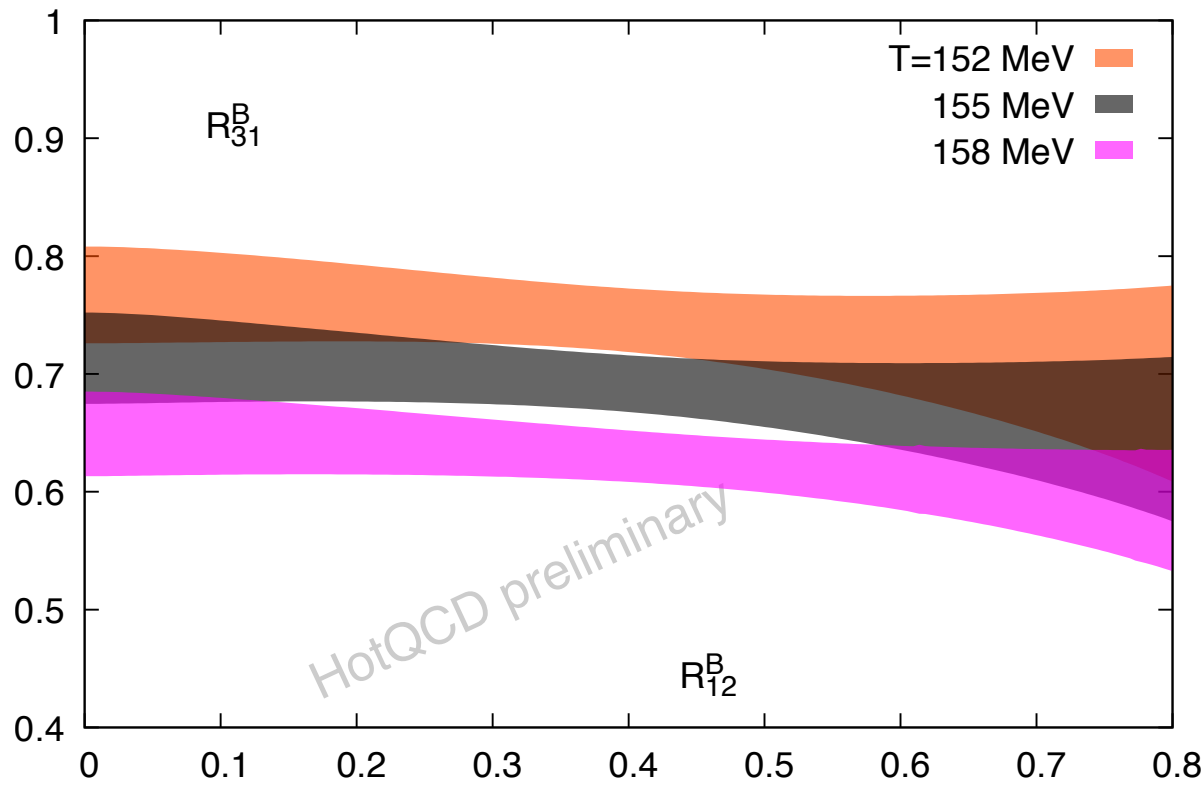
- Skewness and kurtosis ratios R_{31}^B and R_{42}^B on $(N_\tau = 8)$ -lattices



- Convergence gets worth with increasing order of the cumulant and with decreasing temperature.
- NLO and NNLO corrections are negative.

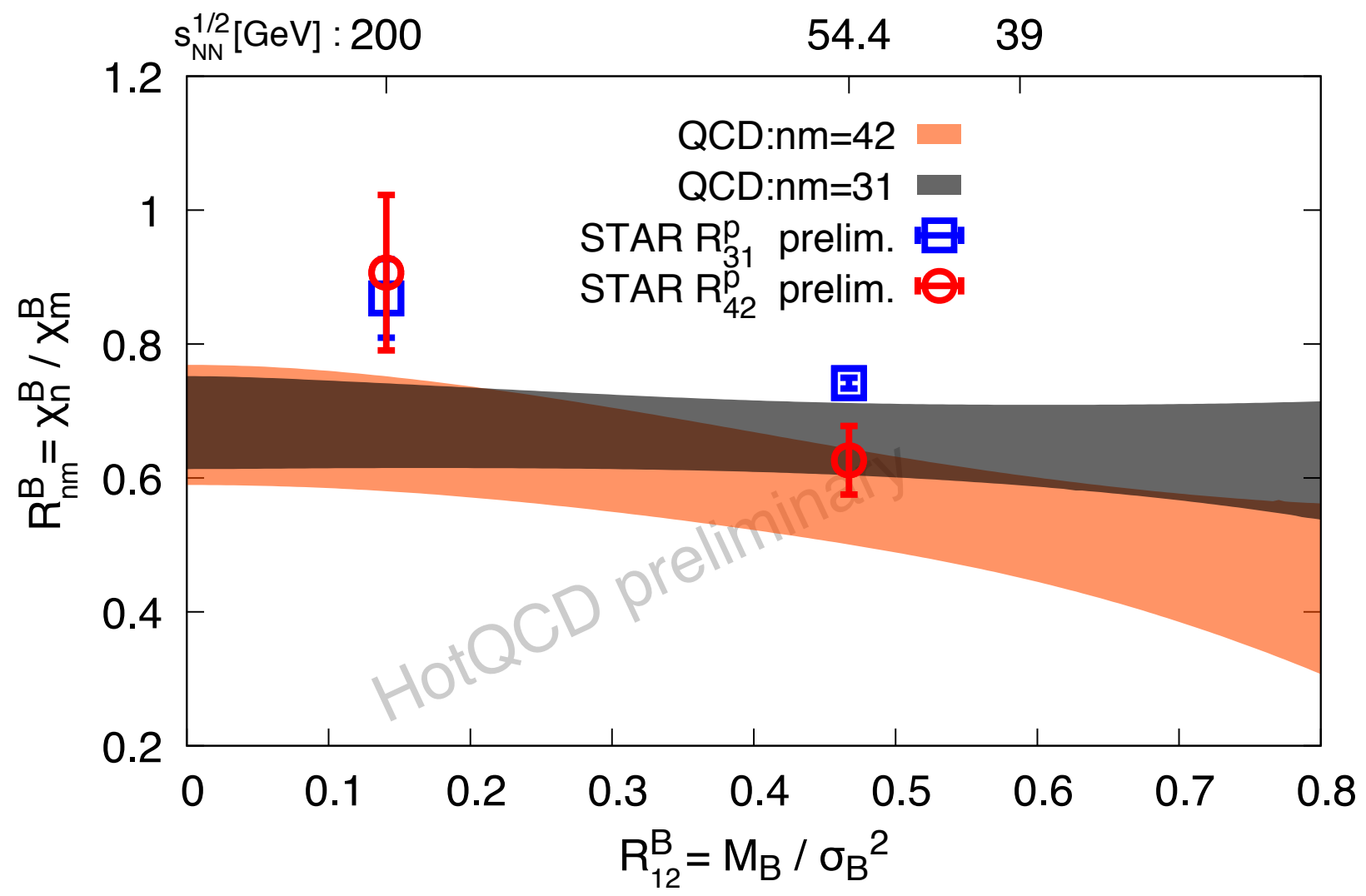
Results: Skewness and kurtosis

- Continuum estimates of R_{31}^B and R_{42}^B as function of R_{12}^B for various temperatures.



- Ratios drop with increasing R_{12}^B and with increasing temperature.

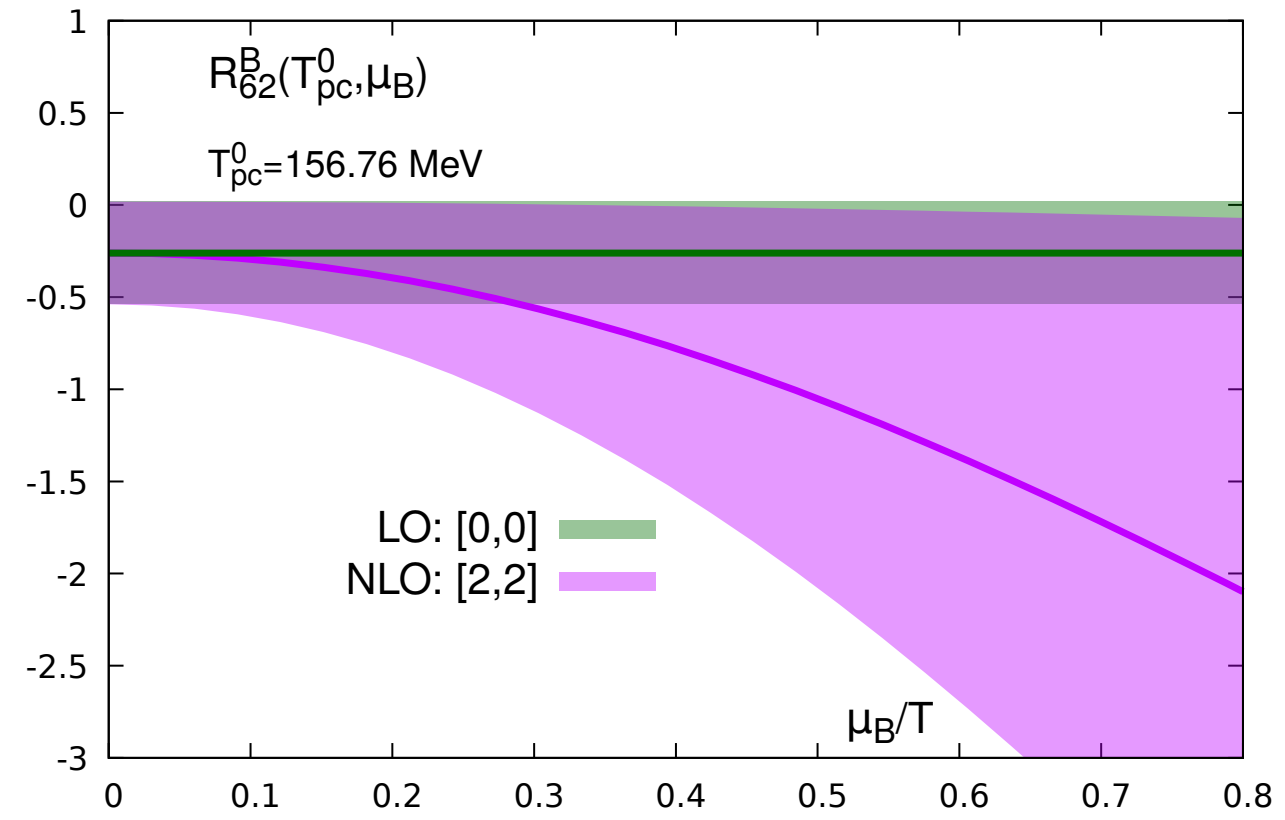
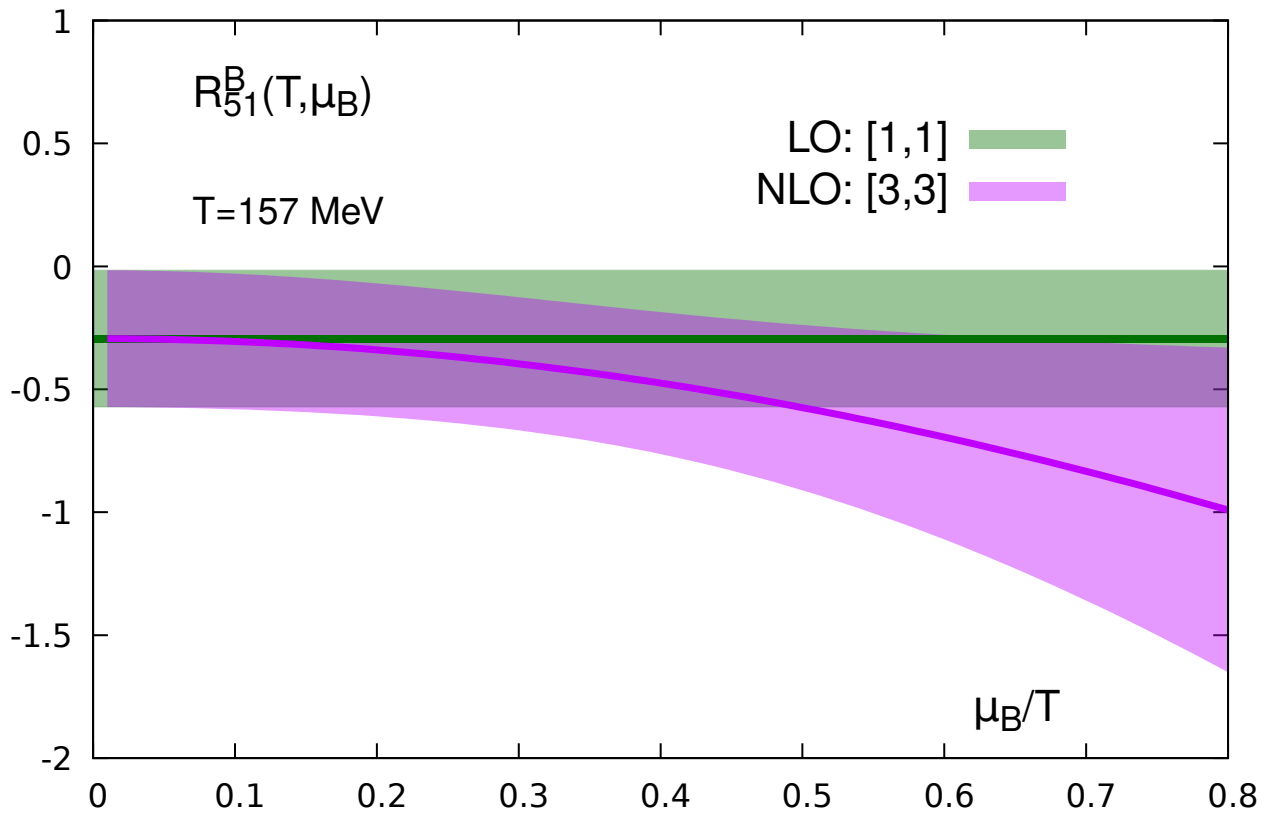
Results: Skewness and kurtosis



- Continuum estimates of R_{31}^B and R_{42}^B as function of R_{12}^B on the crossover line.
- Star data at $\sqrt{s_{NN}} = 54.4$ GeV favors a freeze-out temperature slightly below the crossover.
- The estimate of the freeze-out temperature $T_f = 165$ MeV for $\sqrt{s_{NN}} = 200$ GeV (from a statistical model analysis) is not consistent with a determination of T_f from the skewness and kurtosis data by STAR.

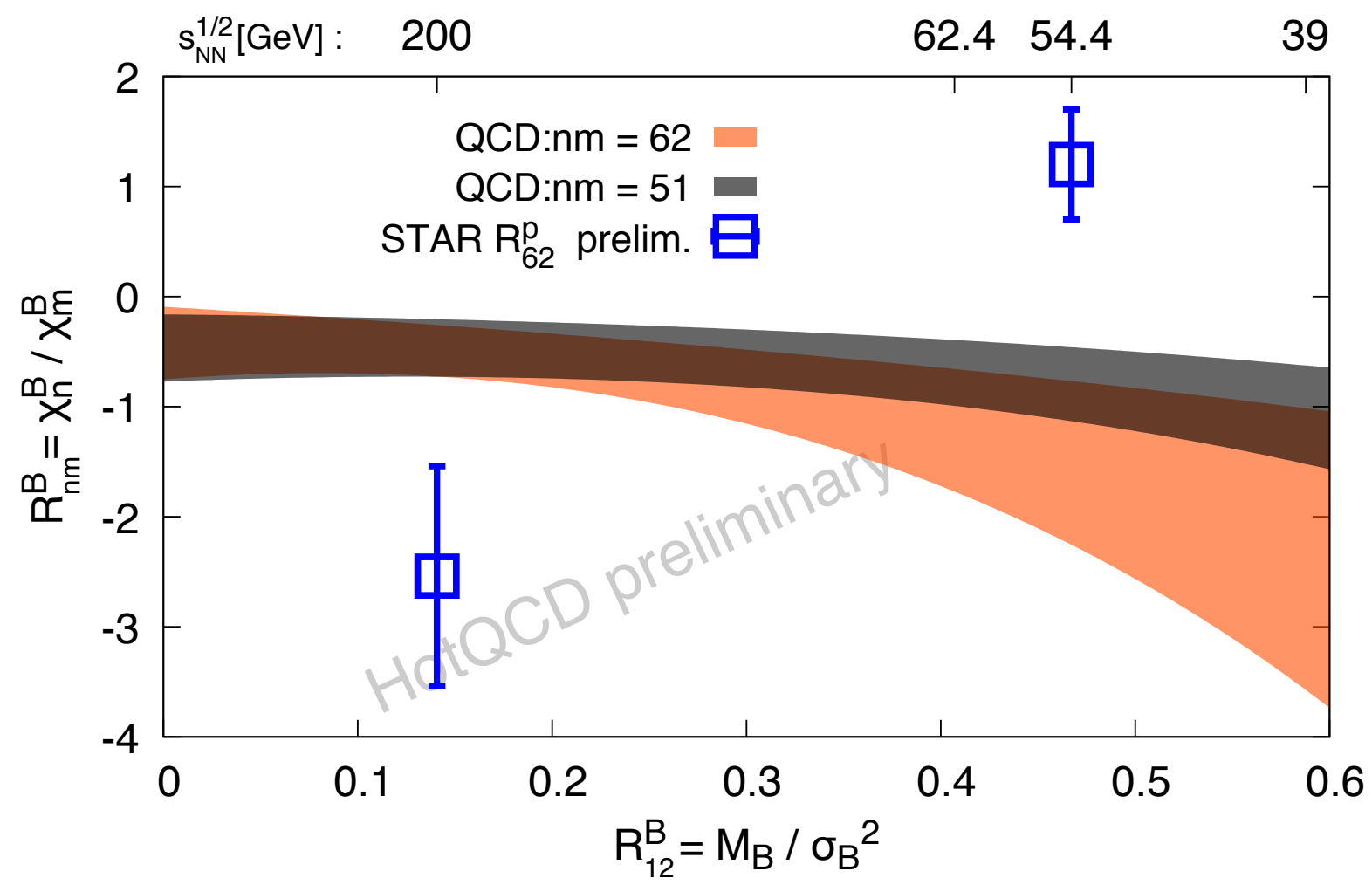
Results: Fifth and sixth order cumulant ratios R_{51}^B and R_{62}^B

● R_{51}^B and R_{62}^B on ($N_\tau = 8$)-lattices



- Large statistical uncertainties
- NLO corrections are negative

Results: Fifth and sixth order cumulant ratios R_{51}^B and R_{62}^B



- R_{51}^B and R_{62}^B on ($N_\tau = 8$)-lattices

- Not consistent with STAR data:

- ➔ A. Pandav@SQM19

$$\sqrt{s_{NN}} = 200 \text{ GeV: } R_{62}^P < 0$$

$$\sqrt{s_{NN}} = 54.4 \text{ GeV: } R_{62}^P > 0$$

- ➔ Lattice QCD predictions

$\sqrt{s_{NN}}$	R_{51}^B	R_{62}^B
200	-0.5(3)	-0.7(3)
54.4	-0.7(4)	-2(1)

Summary and outlook

- Lattice QCD calculators show significant increase in precision for cumulant ratios along the crossover (or any other) line in the QCD phase diagram for $\mu_B/T \leq 1.2$ due to increase in the statistics and thus also the order of the expansion.
- Presented first calculations of R_{51}^B and R_{62}^B along the crossover line
- Freeze-out temperature at $\sqrt{s_{NN}} = 200$ GeV seems not consistent with higher order cumulants
- At $\sqrt{s_{NN}} = 54.4$ GeV we find thermodynamic consistency of the STAR data except for the R_{62}^P data.
- **Outlook:**
 - ▶ Need to increase statistics for $(N_\tau = 12)$ - and $(N_\tau = 16)$ -lattices further.
 - ▶ Need to perform similar analysis for net-electric charge fluctuations, thus need larger volumes.

